Deep-level transient spectroscopy and electrical characterization of ion-implanted *p-n* junctions into undoped InP

Jaime M. Martin, S. García, I. Mártil, and G. González-Díaz
Departamento de Electricidad y Electrónica, Facultad de Ciencias Físicas, Universidad Complutense, 28040 Madrid, Spain

E. Castán and S. Dueñas
Departamento de Electricidad y Electrónica, Facultad de Ciencias, Universidad de Valladolid, 47011 Valladolid, Spain

(Received 19 May 1995; accepted for publication 19 July 1995)

Current-voltage, small-signal measurements, and deep-level transient spectroscopy (DLTS) spectra of *p-n* junctions made by Mg implantation into undoped InP are described. The *I-V* characteristics show that the dominant conduction mechanism at forward bias is recombination in the space-charge zone, whereas a thermally activated tunneling mechanism involving a trap at 0.32 eV dominates at reverse bias. Five deep levels located in the upper-half of the band gap were detected in the junctions by DLTS measurements, three of which (at 0.6, 0.45, and 0.425 eV) were found to appear due to rapid thermal annealing. The origin of the other two levels, at 0.31 and 0.285 eV, can be ascribed to implantation damage. Admittance spectroscopy measurements showed the presence of three levels at 0.44, 0.415, and 0.30 eV, all in agreement with those found by DLTS. The DLTS measurements showed that the concentration of deep levels decreased after longer annealing times, and that the concentration of deep levels due to the implantation increased after additional P or Si implantations. This explains the influence of annealing time and additional implantations on the *I-V* characteristics of the junctions.

I. INTRODUCTION

InP is extensively used for high-frequency and optoelectronic device applications due to its high electron mobility, high thermal conductivity, and direct band gap. Ion implantation combined with rapid thermal annealing (RTA) has proved to be an effective technology for the doping of InP, resulting in high dopant activations and excellent crystalline quality. It also allows for good control of the profiles, especially in the case of *n*-type layers.[1-4] However, the use of these layers in device fabrication requires knowledge of properties that are more specific than those cited above, particularly knowledge concerning the possible formation of deep levels which could degrade device performance. This information is usually obtained from optical (usually photoluminescence) techniques but, in the references cited above, never from electrical measurements when some additional kind of device (a Schottky diode, *p-n* junction, etc.) has to be made.

Most of the literature devoted to the study of *p-n* junctions made by ion implantation into InP deals only with the dc or optoelectronic characterization of the junctions, which are considered as IMPATT diodes,[5] photodiodes,[6] solar cells,[7] waveguides,[8] or as part of junction field-effect transistors (JFETs).[9,10] However, very few results can be found regarding small-signal characterization,[11,12] in spite of the important information that such measurements reveal for devices that will normally be used in high-frequency applications.

In this study, we present the *I-V*, small-signal admittance spectroscopy (AS), and deep-level transient spectroscopy (DLTS) characterizations of *p-n* junctions made by Mg implantation into InP. The former technique gives information about the conduction mechanisms dominating in both forward and reverse bias. Both DLTS and AS were used to look for possible traps formed in the junction due to the implantation or the RTA treatment. Junctions made using Mg and P coimplantation to obtain the p^+-type layer, and an additional Si implantation to increase the carrier concentration in the *n*-type layer, were also characterized in order to study the effect of these additional implantations on the conduction mechanisms or the deep levels.

II. EXPERIMENT

The substrates used in this study were (100)-oriented liquid-encapsulated-Czochralski-grown undoped InP ($n \approx 2\times10^{15}$ cm^{-3}) from a MCP Ltd. The top p^+ layers were formed by Mg implantation at 80 keV with a dose of 10^{14} cm^{-2}, and the effect of phosphorous coimplantation was studied using implantations at 120 keV with a dose of 10^{14} cm^{-2}, which results in profiles that overlap those of Mg. Si was also implanted at 400 keV with a dose of 10^{13} cm^{-2} (the parameters typical for the channel formation of JFETs) to obtain fully ion-implanted junctions. All implantations were performed at room temperature with the substrates tilted 7° off the (100) direction to avoid channeling.

The samples were annealed by RTA using a commercial system from MPT Corp. equipped with a graphite susceptor. The annealing cycles used were 875 °C for 5 or 10 s, which resulted in layers with excellent crystalline quality.[13-15] For junctions formed with an additional Si implantation to increase the carrier concentration in the *n*-type zone, a single RTA treatment was used to activate both the *n*- and *p*-type implants simultaneously.

Ohmic contacts for the n- and p^+-type layers were formed using evaporated AuGe/Au and AuZn/Au, respectively, alloyed at 420 °C for 2 min. The junctions were defined by conventional photolithographic methods with various areas. The results presented here correspond to devices having an area of 400×400 μm^2 (1.6×10^{-3} cm^2). Isolation between devices was obtained by mesa etching using a solution of $1H_2O_2:1H_3SO_4$.

The DC characteristics were measured using a computer-controlled system consisting of a Keithley 230 voltage source, a Keithley 182 precision voltmeter, and a Keithley 2001 multimeter used as an ammeter. The precision of the ammeter was better than 1 nA.

The small-signal ac characterization was performed by AS and DLTS measurements. A Hewlett–Packard 4284A impedance analyzer, with a frequency range from 20 Hz to 1 MHz and a precision better than 1 fF was used for the AS measurements, always with a 50 mV ac signal at 0 V bias. The DLTS measurements were performed using a Boonton 72B capacitance meter and a digital oscilloscope HP-54501A to record the complete transient. The devices were biased at −2 V with a Keithley 617 dc source/electrometer, with filling pulses from −2 to 0 V introduced by a HP214B pulse generator.

III. RESULTS

A. *I-V* characteristics

The study of the p-type layers made by Mg implantation into InP:Fe showed that the hole concentrations for the implantations and the annealing cycles used to make the junctions were in the mid-10^{18} cm^{-3} range.[13] The forward I-V characteristics of all junctions showed ideality factors of $n=2.0$, demonstrating that the main conduction mechanism at forward bias is the recombination in the space-charge zone, which is typical of high band-gap materials. The reverse saturation currents calculated from the forward characteristics were in the range of 10^{-7} A cm^{-2}, with very weak dependence on the RTA cycle or on the use of P coimplantation. The series resistances obtained were lower than 3 Ω. The junctions made with additional Si implantation also resulted in ideality factors of $n=2.0$, but much higher reverse saturation currents (in the range of 10^{-6} A cm^{-2}), which will be discussed in Sec. IV.

Figure 1 shows the temperature dependence of the forward I-V characteristics for a junction made by Mg/P implantation annealed at 875 °C for 10 s. The diode factor was $n=2.00$ down to 183 K, and the reverse saturation current showed a temperature dependence with an activation energy of 0.75 eV, close to the $E_g/2$ expected for a recombination mechanism.[16] At temperatures lower than 180 K the diode factor began to decrease. This same result was obtained for all junctions.

The reverse I-V characteristics of these junctions showed a much clearer dependence than the forward characteristics on the annealing time or the use of additional P or Si implantations. Figure 2 shows the reverse I-V characteristics for junctions made with Mg or Mg/P coimplantation and annealing cycles of 875 °C for 5 or 10 s. As can be seen, the effect of P coimplantation was to increase the reverse current, while the use of longer annealing times decreased the reverse conduction. The junctions made with an additional Si implantation showed a much higher reverse current, as was expected from the forward characteristics.

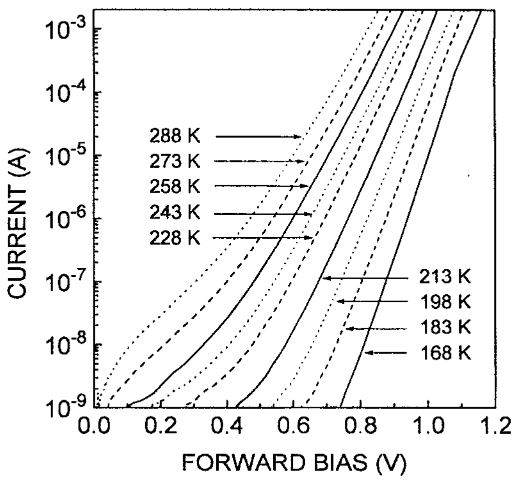

FIG. 1. Forward I-V characteristics at different temperatures for a junction made by Mg/P coimplantation into undoped InP, after RTA at 875 °C for 10 s.

The reverse characteristics of all junctions showed weak temperature dependence, an indication that tunneling should be the dominant mechanism. As in the case of the junctions made into Fe-doped semi-insulating material,[17] a thermally activated tunneling mechanism was used to fit the reverse characteristics, as none of the better-known tunneling mechanisms (such as band to band tunneling or trap assisted tunneling) was found to reproduce the measurements. The expression for this mechanism is[18–20]

$$I_{tt}=KAN_t \exp\left(-\frac{E_t}{kT}\right)\int_0^{\epsilon_t}\exp\left[\epsilon-\frac{C}{E}\epsilon^{3/2}\right]d\epsilon, \qquad (1)$$

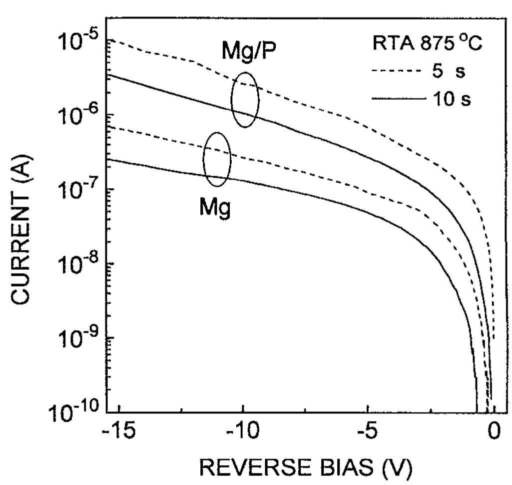

FIG. 2. Reverse I-V characteristics for junctions made by Mg implantation or Mg/P coimplantation, annealed using RTA cycles of 875 °C for 5 or 10 s.

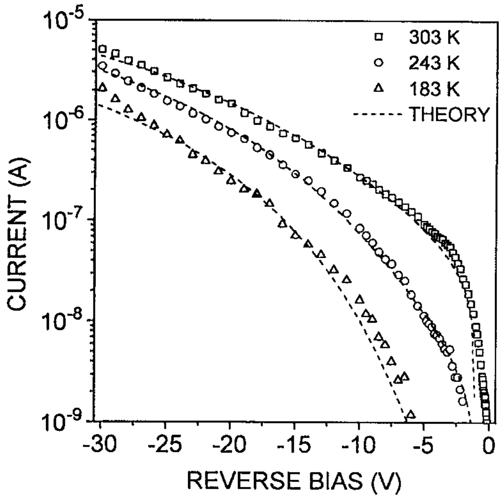

FIG. 3. Reverse I-V characteristics at different temperatures (183, 243, and 303 K) for a junction made by Mg implantation and RTA at 875 °C for 5 s, with the fittings obtained using a thermally activated tunneling mechanism shown by the dashed lines.

where K is a constant, A the junction area, N_t the trap concentration, E_t its energy, E the electric field in the junction, $\epsilon = E/kT$, and

$$C = \frac{8\pi m_t^{1/2}(kT)^{3/2}}{3qh} \qquad (2)$$

with m_t the mass of the carriers in the trap.

Figure 3 shows the fit of this expression to the reverse characteristics at three different temperatures for a junction made by Mg implantation and annealed at 875 °C for 5 s. The parameters obtained from the simulation were $C = 1.0$ and $E_t = 0.32$ eV. It can be seen that this mechanism closely follows the characteristics over a wide range of temperatures and currents, with only a small deviation at low currents, probably due to the appearance of other conduction mechanisms in parallel.

B. DLTS

DLTS[21] is a technique widely used to characterize deep levels in semiconductors, and consists of the measurement of transients in the junction capacitance when a positive bias pulse is applied to a reverse-biased Schottky or p-n junction. In this work, the measurements were performed with the junctions initially at -2 V bias, with filling pulses to 0 V, and involved a region on the n side of the junction extending between 1.5 and 2 μm from the junction. The intensities of DLTS spectra can give information about the deep-level concentrations in the junction, although they must be treated with caution because of the different nonideal effects that can take place in the space-charge region (nonexponential transients, high or nonhomogeneous deep-level concentrations, trap refilling at the edge zone, etc.).[22-25] In spite of this, it should be noticed that the area of all the junctions studied was the same, which allows us to at least derive qualitative trends from direct comparison of the spectra from different junctions.

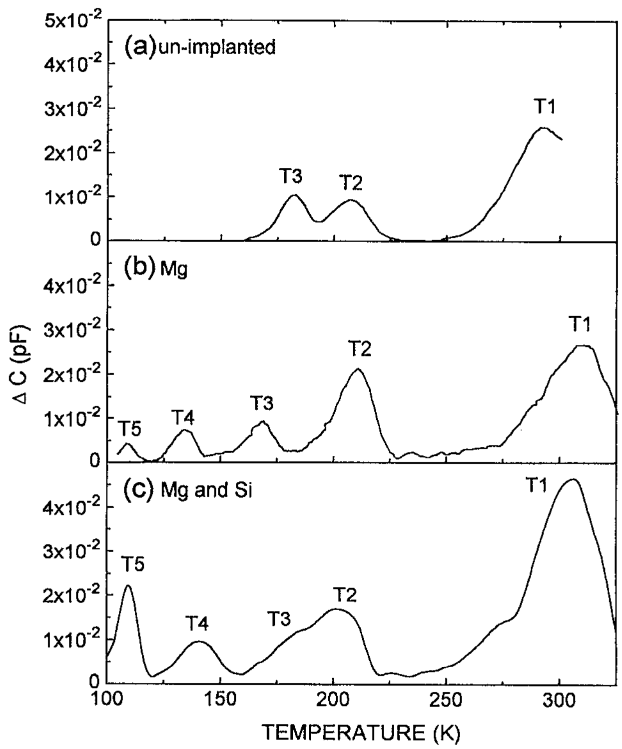

FIG. 4. DLTS spectra (rate window of 57.7 ms) from (a) unimplanted RTA treated (875 °C for 10 s) undoped InP, and from p-n junctions into undoped InP made by (b) Mg implantation (80 keV, 10^{14} cm^{-2}) or (c) Mg and Si implantation (80 keV, 10^{14} cm^{-2}/400 keV, 10^{13} cm^{-2}), all after RTA at 875 °C for 10 s.

Figure 4(a) shows the DLTS spectra of unimplanted RTA-treated InP, obtained using a Schottky junction made by Au evaporation, and those of junctions made by Mg implantation [part (b)] and Mg/Si implantation [part (c)], all annealed with the same RTA cycle (875 °C for 10 s). The virgin material did not show any deep level, while it is clear from Fig. 4(a) that after RTA at 875 °C for 10 s, three levels appeared, labeled T1, T2, and T3 at 0.6, 0.45, and 0.425 eV, respectively (with the energy given from the conduction band). All three levels were electron traps. In the junctions made by ion implantation, two more levels, in addition to T1–T3, were formed, labeled T4 and T5 at 0.31 and 0.285 eV, respectively. The intensity of these two peaks in the junction made with an additional Si implantation [Fig. 4(c)] was larger compared to the case of the junction made only by Mg implantation [Fig. 4(b)]. This is an indication that the implantation is the origin of these levels.

Figure 5 shows the effect of P coimplantation on the DLTS spectra. As can be seen, all levels from T1 to T5 appeared in the spectrum of the junction made with the additional P implantation, and all of them had higher intensities than in the case of the junction made without the P coimplantation.

In Fig. 6, the effect of annealing time (5 or 10 s) on the DLTS spectrum is displayed for a junction made by Mg implantation, where all the levels from T1 to T5 again appeared in both spectra. The intensities of T1, T3, and T4 decreased

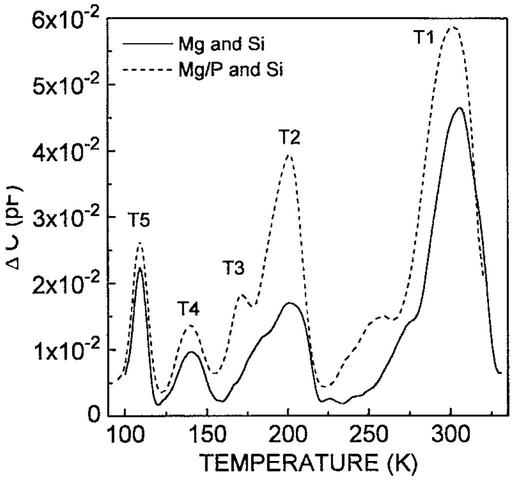

FIG. 5. DLTS spectra (rate window of 57.7 ms) from junctions made by Mg (80 keV, 10^{14} cm^{-2}) and Si (400 keV, 10^{13} cm^{-2}) implantations, with or without additional P coimplantation (120 keV, 10^{14} cm^{-2}), all after RTA at 875 °C for 10 s.

after longer annealing times, while the levels T2 (0.45 eV) and T5 (0.285 eV) were more thermally stable.

C. Admittance spectroscopy

AS[26] measurements at 0 V bias were also performed on the junctions, which would give information about the traps at that point in the space-charge region where the Fermi level crosses the energy of the deep levels. This point is close to the space-charge-region edge (within a debye length of it, that is, around 0.2 to 0.3 μm), so that the information obtained from AS measurements comes from a region closer to the junction than that scanned by the DLTS measurements discussed above.

Figures 7(a) and 7(b) show the results of these measurements for a junction made by Mg implantation and annealed at 875 °C for 10 s. Figure 7(a) presents the capacitance of the

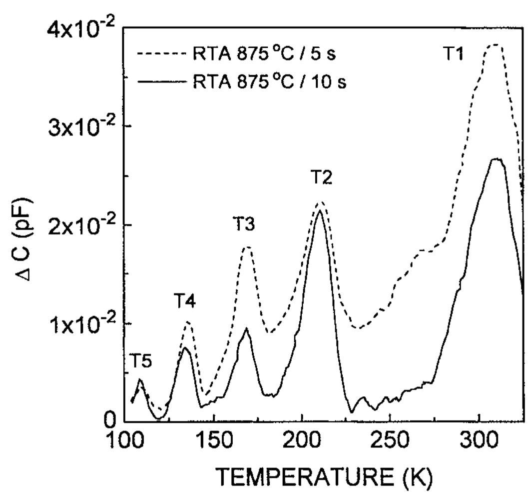

FIG. 6. DLTS spectra (rate window of 57.7 ms) from junctions made by Mg implantation into undoped InP, after RTA at 875 °C for 5 or 10 s.

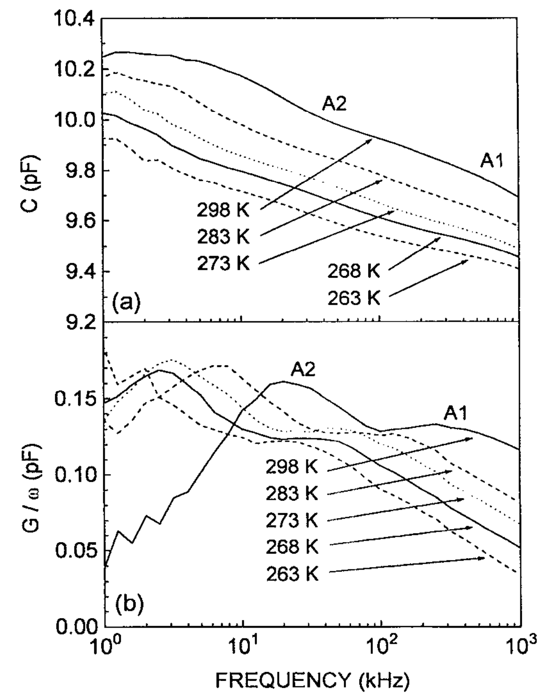

FIG. 7. Admittance spectroscopy measurements (Capacitance and G/ω) for a junction made by Mg implantation (80 keV, 10^{14} cm^{-2}) into InP, after RTA at 875 °C for 10 s.

junction as a function of frequency for several temperatures, where two relaxations can be seen in the capacitance, A1 and A2. The G/ω diagram showed in Figure 7(b) presents these relaxations more clearly. Using the theoretical expressions developed for AS,[27–29] the relaxations in capacitance can be associated with deep levels at 0.415 and 0.44 eV for A1 and A2, respectively. In a similar way, a level at 0.30 eV (A3) was found in the junctions annealed at 875 °C for 5 s.

IV. DISCUSSION

Several authors have already reported the appearance of deep levels in virgin material after a RTA treatment,[30–33] such as those found by us, and labeled T1, T2, and T3 in Figs. 4–6. Regarding the origin of T1 at 0.6 eV, Fe is an impurity present in undoped InP, and it is known to introduce a deep acceptor at an energy of 0.6–0.65 eV,[19] which matches the energy of T1. The fact that it appeared only after the RTA treatment and was not present in the starting material could be due to the well-known effect of Fe outdiffusion during high temperature processes,[34] resulting in an increase in concentration at the surface.

The levels T2 and T3 at energies of 0.45 and 0.425 eV, respectively, could be P vacancies (V_P) or complexes with V_P, which are the most probable defects created in InP after annealing.[35] In fact, Kim *et al.*[31] found a similar level in bulk InP (at 0.43 eV) after treating the material with RTA at 700 °C for 20 s, which they related to V_P, as did Yamamoto *et al.*[36] in metalorganic chemical vapor deposition-InP and Iliadis *et al.*[37] in molecular beam epitaxy-InP. The higher intensity of levels T2 and T3 in the junctions made with P

TABLE I. Energy, capture cross section, and possible origin for the deep levels detected by DLTS measurements in the junctions made by ion implantation into undoped InP.

Level	Energy (eV)	Capture cross section (cm^2)	Possible origin
T1	0.6	4.6×10^{-13}	Fe contamination
T2	0.45	3.4×10^{-14}	V_P related
T3	0.425	4.2×10^{-12}	
T4	0.31	6.9×10^{-14}	Implantation damage
T5	0.285	1.9×10^{-15}	(probably V_{In} related)

coimplantation (see Fig. 5) could be surprising at first, since the additional P should decrease the concentration of all defects related to V_P. However, it should be noticed that the region measured by both DLTS and AS is the n-type zone, while the P is co-implanted overlapping the Mg profile in the p-type region of the junction.

The origin of levels T4 and T5 (at 0.31 and 0.285 eV, respectively) is clearly the implantation, as none of these levels appeared in the virgin material or the material treated by RTA, but were present in all the junctions made by ion implantation. The additional implantations with P or Si increased the intensity of these levels, which points to an intrinsic defect produced by radiation damage as their most probable origin. Kringhoj[12] found electron traps at 0.28 and 0.45 eV in n^+-p junctions made in InP by Ge implantation and RTA, both of which could be the same as found by us. Kruppa *et al.*[38] reported a frequency dispersion in the gain of a fully ion-implanted InP JFET with an activation energy of 0.28 eV, which could also be related to one of these levels. The dominant intrinsic defects in n-type InP are predicted to be V_{In} (In vacancies) and In_P (antisites).[39] However, from photoluminescence measurements Thompson *et al.*[40] related a deep center close to the middle of the gap (at 0.75 eV from the conduction band) to In_P antisites, far from the energies of 0.3 eV found by us, which would suggest V_{In} as the most probable defect related to these levels.

A summary of these results is given in Table I, which shows the deep levels detected from DLTS measurements, the capture cross-sections obtained, and an indication of their possible origin. The corresponding concentrations were in the range of 10^{12}–10^{13} cm^{-3}.

The dependence of the I-V characteristics on additional Si or P implantations and on annealing time can be explained from Figs. 4, 5, and 6, respectively. The higher concentration of traps in the junctions made with additional Si or P implantations (Figs. 4 and 5) is responsible for the higher reverse saturation currents of these junctions compared to those of the junctions made only with Mg implantation as, both in the case of recombination (forward bias) or tunneling (reverse bias), the current is proportional to the trap concentration.[16] This same effect explains the dependence on annealing time of the reverse characteristics (Fig. 2), as after annealing for 10 s there is a clear decrease in the trap concentration compared to the case of the junctions annealed for only 5 s.

It is also interesting to notice the excellent agreement between DLTS and AS measurements in three of the levels (T2, T3, and T4), for which the energies obtained by both techniques were almost the same, in all cases within the experimental error. Regarding the dc measurements, where a level at 0.32 eV was used to fit the reverse I-V characteristics, this level could be the same one found at 0.31 eV by DLTS and at 0.30 eV by AS. The fact that this level, and not another one of higher intensity in the DLTS spectra (such as T1, T2, or T3), governs the reverse characteristics of the junctions up to a reverse bias of 30 V indicates clearly that the level T4 at 0.31 eV must be the most abundant at a long distance from the junction. A detailed study of the concentration depth profiles of these levels is currently underway using the capacitance-voltage transient technique,[41] which we hope will help to clarify this point.

V. CONCLUSIONS

The dc and ac characteristics, and the DLTS spectra of ion implanted p-n junctions in undoped InP have been presented in this study. The forward characteristics were dominated by the recombination mechanism, while a thermally activated tunneling mechanism correctly explains the reverse characteristics, with a trap at 0.32 eV.

DLTS and AS showed the presence of several deep levels in the junctions at energies of 0.6 eV, 0.45 eV (or 0.44 eV, from AS measurements), 0.425 eV (0.415), 0.31 eV (0.30), and 0.285 eV. The level at 0.6 eV could be related to Fe, and those at 0.45, and 0.425 eV were found to appear just after a RTA treatment, being most probably related to V_P. The other two levels at 0.31 and 0.285 eV appeared only in the p-n junctions made by implantation, and their origin could be related to an intrinsic defect in n-type InP, probably V_{In}. The intensity of these levels increased after additional P or Si implantations and decreased after longer annealing times. These are variations that we have used to explain the I-V characteristics.

ACKNOWLEDGMENTS

The authors thank the Centro de Investigación y Desarrollo de la Armada (CIDA) for assistance with lithography. This work has been partly supported by Project No. TIC93/175 of the spanish CICYT.

[1] M. V. Rao, Appl. Phys. Lett. **48**, 1522 (1986).
[2] M. V. Rao and P. E. Thompson, Appl. Phys. Lett. **50**, 1444 (1987).
[3] H. Shen, G. Yang, Z. Zhou, and S. Zou, Appl. Phys. Lett. **56**, 463 (1990).
[4] T. D. Thompson, J. Barbara, and M. C. Ridgway, J. Appl. Phys. **71**, 6073 (1992).
[5] J. J. Berenz, F. B. Fank, and T. L. Hierl, Electron. Lett. **14**, 684 (1978).
[6] C. A. Armiento, J. P. Donnelly, and S. H. Groves, Appl. Phys. Lett. **34**, 229 (1979).
[7] C. J. Keavney and M. B. Spitzer, Appl. Phys. Lett. **52**, 1439 (1988).
[8] K. Oigawa, S. Uekusa, Y. Sugiyama, and M. Tacano, Jpn. J. Appl. Phys. **25**, 1902 (1986).
[9] S. J. Kim, K. W. Wang, G. P. Vella-Coleiro, J. W. Lutze, Y. Ota, and G. Guth, IEEE Electron Device Lett. **EDL-8**, 518 (1987).
[10] J. B. Boos, W. Kruppa, and B. Molnar, IEEE Electron Device Lett. **EDL-10**, 79 (1989).
[11] A. L. Conjeaud, B. Orsal, A. Dhouib, R. Alabedra, and L. Gouskov, J. Appl. Phys. **59**, 1707 (1986).
[12] P. Kringhoj, Mater. Sci. Eng. B **9**, 315 (1991).

[13] J. M. Martin and G. González-Díaz, Nucl. Instrum. Methods B **88**, 331 (1994).
[14] J. M. Martin, S. García, F. Calle, I. Mártil, and G. González-Díaz, J. Electron. Mater. **24**, 59 (1995).
[15] J. M. Martin, S. García, I. Martil, G. González-Díaz, R. Cuscó, and L. Artús, *Proceedings of the First International Conference on Materials for Microelectronics* (The Institute of Materials, Barcelona, 1994), p. 17.
[16] S. M. Sze, *Physics of Semiconductor Devices* (Wiley, New York, 1981).
[17] J. M. Martin, S. García, I. Mártil, and G. González-Díaz (unpublished).
[18] G. Vincent, A. Chantre, and D. Bois, J. Appl. Phys. **50**, 5484 (1979).
[19] J. Cheng, S. R. Forrest, B. Tell, D. Wilt, B. Schwartz, and P. Wright, J. Appl. Phys. **58**, 1787 (1985).
[20] W. Haussler and D. Romer, J. Appl. Phys. **67**, 3400 (1990).
[21] D. V. Lang, J. Appl. Phys. **45**, 3023 (1974).
[22] W. R. Thurber, R. A. Forman, and W. E. Philips, J. Appl. Phys. **53**, 7397 (1982).
[23] P. Omling, L. Samuelson, and H. G. Grimmeiss, J. Appl. Phys. **54**, 5117 (1983).
[24] P. M. Mooney, T. N. Theis, and S. L. Wright, Appl. Phys. Lett. **53**, 1546 (1988).
[25] L. Enríquez, S. Dueñas, J. Barbolla, I. Izpura, and E. Muñoz, J. Appl. Phys. **72**, 525 (1992).
[26] J. Barbolla, S. Dueñas, and L. Bailón, Solid-State Electron. **35**, 285 (1992).
[27] D. L. Loose, Appl. Phys. Lett. **21**, 54 (1972).
[28] D. L. Loose, J. Appl. Phys. **46**, 2204 (1975).
[29] J. L. Pautrat, B. Katircioglu, N. Magnea, D. Bensahel, J. C. Pfister, and L. Revoil, Solid State Electron. **23**, 1159 (1980).
[30] J. K. Luo, T. Kimura, S. Yugo, and Y. Adachi, Jpn. J. Appl. Phys. **26**, 82 (1987).
[31] E. K. Kim, H. Y. Cho, J. H. Yoon, S. Min, Y. L. Jung, and W. H. Lee, J. Appl. Phys. **68**, 1665 (1990).
[32] C. S. Ma, P. W. Chan, V. C. Lp, C. W. Ong, and S. P. Wong, J. Electron. Mater. **23**, 459 (1994).
[33] K. L. Liao, A. J. Soltyka, W. A. Anderson, and A. Katz, Appl. Phys. Lett. **57**, 1913 (1990).
[34] S. J. Pearton and A. Katz, Mater. Sci. Eng. B **18**, 153 (1993).
[35] J. D. Oberstar and B. G. Streetman, Thin Solid Films **103**, 17 (1983).
[36] N. Yamamoto, K. Uwai, and K. Takahei, J. Appl. Phys. **65**, 3072 (1989).
[37] A. A. Iliadis, S. C. Laith, and E. A. Martin, Appl. Phys. Lett. **54**, 1436 (1989).
[38] W. Kruppa, J. B. Boos, and T. F. Carruthers, *Proceedings of the Third International Conference on InP and Related Materials* (IEEE, New York, 1991), IEEE Catalog #91CH2950-4.
[39] R. W. Jansen, Phys. Rev. B **41**, 7666 (1990).
[40] T. D. Thompson, J. Barbara, and M. C. Ridgway, J. Appl. Phys. **71**, 6073 (1992).
[41] S. Dueñas, E. Castán, L. Enríquez, J. Barbolla, J. Montserrat, and E. Lora-Tamayo, Semicond. Sci. Technol. **9**, 1637 (1994).